

## Peptide-Mediated Cellular Uptake of Cryptophane

Garry K. Seward, Qian Wei, and Ivan J. Dmochowski

*Bioconjugate Chem.*, **2008**, 19 (11), 2129-2135 • DOI: 10.1021/bc8002265 • Publication Date (Web): 17 October 2008

Downloaded from <http://pubs.acs.org> on February 4, 2009

### More About This Article

---

Additional resources and features associated with this article are available within the HTML version:

- Supporting Information
- Links to the 1 articles that cite this article, as of the time of this article download
- Access to high resolution figures
- Links to articles and content related to this article
- Copyright permission to reproduce figures and/or text from this article

[View the Full Text HTML](#)



# Peptide-Mediated Cellular Uptake of Cryptophane

Garry K. Seward, Qian Wei, and Ivan J. Dmochowski\*

Department of Chemistry, University of Pennsylvania, 231 South 34th Street, Philadelphia, Pennsylvania 19104-6323. Received June 1, 2008; Revised Manuscript Received August 24, 2008

Cryptophane-A has generated considerable interest based on its high affinity for xenon and potential for creating biosensors for  $^{129}\text{Xe}$  nuclear magnetic resonance (NMR) spectroscopy. Here, we report the cellular delivery of three peptide-functionalized cryptophane biosensors. Cryptophanes were delivered using two cationic cell penetrating peptides into several human cancer and normal cell lines. An RGD peptide targeting  $\alpha_v\beta_3$  integrin receptor was shown to increase specificity of cryptophane cell uptake. Labeling the peptides with Cy3 made it possible to monitor cellular delivery using confocal laser scanning microscopy. The peptido-cryptophanes were determined to be relatively nontoxic by MTT assay at the micromolar cryptophane concentrations that are required for  $^{129}\text{Xe}$  NMR biosensing experiments.

## INTRODUCTION

Magnetic resonance imaging (MRI) identifies molecules at high spatial resolution within deep tissue and can facilitate the diagnosis of many diseases. However, MRI suffers from low sensitivity and high background signals due to intrinsic  $^1\text{H}$  signals from water and fat. In MRI procedures involving human subjects, signals are typically enhanced using gadolinium- or iron-oxide-based agents at approximately 0.1 mmol/kg. However, it has been challenging using these contrast agents to identify biomolecular targets, such as proteins, which are typically present in cells at low concentrations (1, 2). Moreover, U.S. and European agencies recently issued advisories regarding the risks posed by gadolinium agents in patients with impaired renal function. These findings motivate studies of non-proton-based, hyperpolarized MRI agents such as  $^{129}\text{Xe}$ ,  $^{13}\text{C}$ , and  $^3\text{He}$ , which enable physiological assays, and provide potentially more sensitive methods for studying proteins and metabolites (3–5).  $^{129}\text{Xe}$  is particularly attractive due to its large chemical shift window and laser polarization of nuclear spins, which enhances  $^{129}\text{Xe}$  NMR signals by more than 10 000-fold. Importantly, the environmental sensitivity of the xenon chemical shift allows the simultaneous detection of multiple species in solution.  $^{129}\text{Xe}$  NMR biosensing has been elegantly demonstrated using a cryptophane organic host molecule that binds xenon and can be targeted to specific analytes in solution (6).

Cryptophanes are versatile host molecules whose size can be tuned to bind xenon and a variety of organic solvents and cationic species (7). In cryptophane-A, two cyclotrimeric cages are joined by three ethylene linkers to form a 1-nm-diameter pseudospherical cage with internal volume of  $\sim 95 \text{ \AA}^3$ . Hill et al. showed that a tricarboxylate-modified cryptophane-A binds xenon with comparable affinity in buffer ( $K_A = 30\,000 \text{ M}^{-1}$ ) and human plasma ( $K_A = 22\,000 \text{ M}^{-1}$ ) at 310 K (8). This avidity for xenon has motivated the design of cryptophane-A biosensors for detecting protein binding (9) or enzyme-related activity (10) by laser-polarized  $^{129}\text{Xe}$  nuclear magnetic resonance (NMR) spectroscopy. Biotin-functionalized cryptophanes produced a 1–4 ppm change in  $^{129}\text{Xe}$  NMR chemical shift upon

streptavidin binding (11–14). Similarly, peptide-decorated cryptophane-A reported cleavage by matrix metalloproteinase-7 (MMP-7), which is secreted from many human tumors (10). Importantly, the cryptophane did little to affect MMP-7 activity, with peptide cleavage producing a 0.5 ppm change in  $^{129}\text{Xe}$  NMR chemical shift. These results motivate the development of cryptophane biosensors for in vivo  $^{129}\text{Xe}$  NMR studies. However, very few water-soluble cryptophanes (15) have been synthesized, and little is known about their biological activity. We are not aware of any cell or animal studies involving cryptophanes that have been reported up to this time. In the current study, we investigated the uptake of peptide-modified cryptophane-A in human cancer, fibroblasts, and red blood cells.

Cryptophane-A has poor (low micromolar) water solubility and a molecular weight of 895 g/mol, which limits spontaneous intracellular diffusion, as can occur with smaller drug-like compounds. Thus, in order to test cryptophane cellular compatibility, one possible delivery method involves the use of polycationic peptides that help to solubilize the cryptophane and are rich in the basic amino acids arginine and lysine. These peptides, known generally as cell penetrating peptides (CPPs), can transport through cell membranes covalently attached cargo such as therapeutics, nucleic acids, and imaging agents (16–19). In one example, porphyrins useful for photodynamic therapy were delivered to cellular compartments by conjugating a segment of the human immunodeficiency transcriptional activator (HIV-1 TAT) or short peptides containing 6–9 consecutive arginines (20). Buckminsterfullerene, which is similar to cryptophane-A in molecular weight and chemical formula, was delivered to HEK-293 cells by attaching oligomers of lysine (21). These studies highlight the utility of CPPs for improving cellular uptake and bioavailability of large organic molecules.

Another cell delivery method involves the specific targeting of cell surface receptors, such as integrins (22–24), somatostatin (25–27), or folate (28). Integrin receptors are overexpressed in a variety of cancer cells and linked to tumor metastasis and invasion (29, 30). It is found that the  $\alpha_v\beta_3$  integrin receptor in particular is substantially up-regulated in fast-growing tumor cells, compared to minimum expression in most normal tissues (31, 32). A cyclic tripeptide RGD sequence is known to target the  $\alpha_v\beta_3$  integrin receptor (ABIR) (33–36). More recently, it was demonstrated that linear multimeric (RGD) $_n$  sequences also target the ABIR and promote the uptake of near-infrared-emitting cyprate in A549 nonsmall cell carcinoma cells (37).

\* To whom correspondence should be addressed. Department of Chemistry, University of Pennsylvania, 231 South 34th St., Philadelphia, PA 19104-6323. E-mail: ivandmo@sas.upenn.edu, Phone: 215-898-6459, Fax: 215-898-2037.

This strategy of selectively delivering biologically active molecules is particularly useful for imaging tumors, which overexpress a large number of cell surface receptors.

In the present study, we report the synthesis of cryptophane-A conjugated to HIV-1 TAT (residues 48–60), a nonamer of D-arginine, or the (RGD)<sub>4</sub> dodecamer. Cell penetrating peptides were chosen to examine initially whether cryptophanes could be delivered to cells and to measure the effects of nonspecific delivery on cell viability. The (RGD)<sub>4</sub> peptide was chosen for its ability to target cells overexpressing ABIR (37). Cysteine incorporation within these peptides provided a route for subsequent labeling with Cy3. Cell uptake and cytotoxicity were measured for AsPC-1 and CAPAN-2 pancreatic cancer cells, HFL-1 human lung fibroblasts, and human red blood cells.

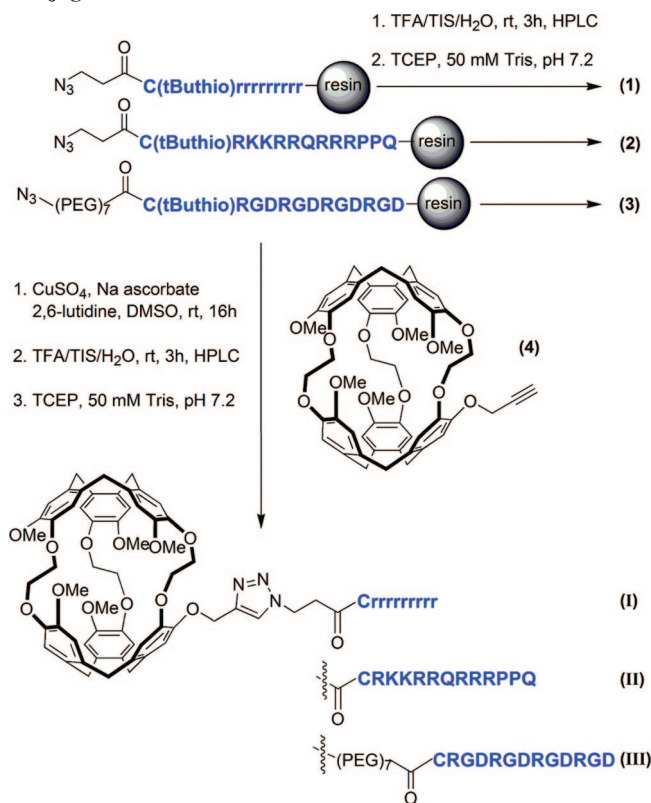
## EXPERIMENTAL PROCEDURES

**Reagents.** Organic reagents and solvents were used as purchased from the following commercial sources: Sigma-Aldrich: dimethyl sulfoxide (DMSO), dimethylformamide (DMF), methanol, triisopropylsilane (TIS), 2,6-lutidine, piperidine, 3-(4,5-dimethyl-2-thiazolyl)-2,5-diphenyl-2*H*-tetrazolium bromide (MTT); Fisher: sodium chloride, copper(II) sulfate, trifluoroacetic acid (TFA), diethyl ether (Et<sub>2</sub>O), glutathione; Alfa Aesar: cesium carbonate, L-glutathione; Novabiochem: 2-(1*H*-benzotriazole-1-yl)-1,1,3,3-tetramethyluronium hexafluorophosphate (HBTU), *N*-methylmorpholine (0.4 M), *O*-(2-azidoethyl)-*O'*-(*N*-diglycolyl-2-aminoethyl)heptaethyleneglycol ((PEG)<sub>7</sub> linker), Rink amide resin, Fmoc-protected amino acids including Fmoc-L-Lys(Boc)-OH, Fmoc-Gly-OH, Fmoc-L-Arg(Pbf)-OH, Fmoc-Gln(Trt)-OH, Fmoc-Cys(tButhio)-OH, Fmoc-L-Pro-OH; GE Healthcare: Cy3 monoreactive dye pack, Sephadex G-25 size exclusion column; Calbiochem: tris(2-carboxyethyl)phosphine hydrochloride (TCEP-HCl), cyclo-Arg-Gly-Asp-D-Phe-Val (cyclo-RGDfV); Invitrogen: RPMI medium 1640, Dulbecco's phosphate buffered saline (DPBS), anti-CD51 mouse antibody; Pierce: Ellman's reagent. For biological assays, all solutions were prepared using deionized water purified by Mar Cor Premium grade Mixed Bed Service Deionization. The standard buffer is defined herein as 50 mM Tris, 5 mM CaCl<sub>2</sub>, 300 mM NaCl, pH 7.2.

**General Methods.** All air- and moisture-sensitive reactions were performed under dinitrogen with glassware oven-dried and then flamed under partial vacuum. Peptides were generated using a Protein Technologies PS3 Peptide Synthesizer. HPLC analysis was performed on an Agilent 1100 system equipped with a quaternary pump and diode array detector using a Zorbax Rx-C8 semipreparative (9.4 × 250 mm, 5 μm) or analytical column (4.6 × 150 mm, 5 μm). The gradient eluent was composed of two solvents: 0.1% aqueous TFA (solvent A) and a 0.1% solution of TFA in CH<sub>3</sub>CN (solvent B). Mass identification of all peptide-containing compounds was performed by the Wistar Institute Proteomics Facility using an Applied Biosystems Voyager 6030 MALDI-TOF mass spectrometer. UV-visible spectra for peptides and peptide-cryptophane-A conjugates were measured using an Agilent 89090A spectrophotometer. Fluorescence spectra were collected for Cy3-labeled peptides dissolved in standard buffer (λ<sub>ex</sub> = 552 nm) using a Varian Cary Eclipse fluorescence spectrophotometer in small volume, 1-cm path length quartz cuvettes at rt (1 nm steps, 5 nm excitation and emission slits). The 96 well fluorescence measurements were made using a Labsystems Fluoroskan II microplate reader.

**Peptide Synthesis and Purification.** Peptides 1–3 (Scheme 1) were prepared by solid-phase synthesis using standard Fmoc amino acid protection chemistry on Rink Amide resin (0.1 mmol scale). Couplings of Fmoc-protected amino acids to the resin were carried out with HBTU and *N*-methylmorpholine to generate the activated ester. The resin was swelled in DMF (10

## Scheme 1. Synthesis of Peptides 1–3 and Peptide–Cryptophane Conjugates I–III<sup>a</sup>



<sup>a</sup> Azido-peptide on solid support was reacted with monopropargyl-cryptophane-A via a Cu(I)-mediated [3 + 2] cycloaddition reaction. (PEG)<sub>7</sub> = -(CH<sub>2</sub>)<sub>2</sub>-O-(CH<sub>2</sub>CH<sub>2</sub>O)<sub>7</sub>-CH<sub>2</sub>CH<sub>2</sub>NHCOCH<sub>2</sub>OCH<sub>2</sub>.

min) prior to synthesis. Amino acids were then added sequentially until 3-azidopropanoic acid was attached at the N-terminus as the final step. All residues were coupled onto resin by the following procedure: removal of Fmoc group (20% piperidine solution in DMF, 2 × 5 min), wash (DMF, 6 × 30 s), activation (amino acid/HBTU/*N*-methylmorpholine, 1 × 30 s) coupling (amino acid/HBTU/*N*-methylmorpholine, 1 × 20 min), rinse (DMF, 3 × 30 s). Cleavage from the resin was accomplished with a mixture of TFA, TIS, and water (90/5/5) at rt for 3 h. The cleavage cocktail removed side chain protecting groups from all amino acids except for cysteine, which was protected by *t*-butylthiol. Semipreparative HPLC purification of all Cys-protected peptides was accomplished with a gradient: time 0, A/B = 100/0; 0–25 min, linear increase to A/B = 75/25; 25–27 min, linear change to A/B = 20/80; 27–37 min, A/B = 20/80. Selective cysteine deprotection was later performed by treating with TCEP (1 equiv) for 30 min, and running the reaction mixture through a NAP-10 gel filtration to remove TCEP.

The peptide sequences prepared were as follows: N<sub>3</sub>-CH<sub>2</sub>CH<sub>2</sub>-CONH-Crrrrrrrr (D-Arg<sub>9</sub>, **1**), N<sub>3</sub>-CH<sub>2</sub>CH<sub>2</sub>-CONH-CGRKKRRQRRRPPQ (TAT, **2**), and N<sub>3</sub>-CH<sub>2</sub>CH<sub>2</sub>O(PEG)<sub>7</sub>-CONH-CRGDRGDRGDRGD (RGD<sub>4</sub>, **3**). MALDI MS calculated for D-Arg<sub>9</sub> peptide, C<sub>60</sub>H<sub>119</sub>N<sub>40</sub>O<sub>12</sub>S<sub>1</sub> (M + H<sup>+</sup>) 1623.97; found 1624.09. MALDI MS calculated for TAT peptide, C<sub>76</sub>H<sub>139</sub>N<sub>39</sub>O<sub>18</sub>S<sub>1</sub> (M + H<sup>+</sup>) 1918.09; found 1919.15. MALDI MS calculated for RGD<sub>4</sub> peptide C<sub>73</sub>H<sub>128</sub>N<sub>29</sub>O<sub>33</sub>S<sub>1</sub> (M + H<sup>+</sup>) 1970.90; found 1971.07. Pure peptides 1–3 were studied as-is, or subsequently conjugated with Cy3.

**Synthesis of Peptide–Cryptophane Conjugates, I–III.** [3 + 2] Cycloaddition reactions between azide-terminated peptides (still attached to solid support) and monopropargylated cryptophane-A **4** were performed to generate the peptide–cryptophane-A conjugates (Scheme 1) following established protocols

(10). Briefly, an aqueous solution of copper (II) sulfate (0.006 mmol, 0.5 equiv) was added to the resin containing azidopeptide (20 mg, maximum 0.0124 mmol azidopeptide, 1 equiv) followed by 2,6-lutidine (2.78 mL, 0.024 mmol, 2 equiv), sodium ascorbate (0.018 mmol, 1.5 equiv), and **4** (21 mg, 0.024, 2 equiv). Monopropargylated cryptophane-A was synthesized as previously described (10). The suspension was degassed with N<sub>2</sub> and stirred at rt for 16 h. The resin was then transferred to a fritted reaction vessel and washed sequentially with CH<sub>2</sub>Cl<sub>2</sub>, MeOH, water, and 1:1 MeOH/CH<sub>2</sub>Cl<sub>2</sub> before drying under vacuum.

Cleavage from the resin was accomplished with a mixture of TFA, TIS, and water (90/5/5) at rt for 3 h. The Cys-protected peptide–cryptophane conjugates were precipitated and washed with anhydrous Et<sub>2</sub>O before drying under vacuum. Analytical HPLC was performed using a gradient: time 0, A/B = 75/25; 0–25 min, linear increase to A/B = 50/50; time 25–27 min, linear change to A/B = 20/80; 27–37 min, A/B = 20/80. HPLC traces and retention times are provided in the Supporting Information. The cysteine was subsequently deprotected with TCEP in order to generate conjugates **I–III** (Scheme 1). MALDI MS calculated for C<sub>116</sub>H<sub>173</sub>N<sub>40</sub>O<sub>24</sub>S<sub>1</sub> (D-Arg<sub>9</sub>-cryptophane, **I**) (M + H<sup>+</sup>) 2542.33; found 2542.08. MALDI MS calculated for C<sub>132</sub>H<sub>193</sub>N<sub>39</sub>O<sub>30</sub>S<sub>1</sub> (TAT-cryptophane, **II**) (M + H<sup>+</sup>) 2836.45; found 2836.96. MALDI MS calculated for C<sub>129</sub>H<sub>182</sub>N<sub>29</sub>O<sub>45</sub>S<sub>1</sub> ((RGD)<sub>4</sub>-cryptophane, **III**) (M + H<sup>+</sup>) 2889.26; found 2889.07. An extinction coefficient for **I–III**, 9300 M<sup>-1</sup> cm<sup>-1</sup> at 280 nm in water, was determined from solutions containing a weighed sample, as described previously (10).

**Cysteine Labeling with Cy3.** The pure Cys-protected peptides and Cys-protected peptide–cryptophane-A conjugates were dissolved in Tris buffer (50 mM, pH 7.2) at a concentration of 60 μM. Cysteine labeling with the Cy3-maleimide construct was performed according to the manufacturer's protocol. As described previously, cysteine was deprotected with TCEP, which was then removed by NAP-10 column. Cy3 dye was added dropwise and reacted for 3 h. The reaction was quenched by addition of glutathione (1 equiv). The reaction mixture was run through a NAP-10 gel filtration column before analytical HPLC purification.

For Cy3-labeled **I–III**, HPLC elution was achieved with the following gradient: time 0, A/B = 75/25; 0–25 min, linear increase to A/B = 50/50; 25–27 min, linear change to A/B = 20/80; 27–37 min, A/B = 20/80. MALDI MS calculated for C<sub>153</sub>H<sub>215</sub>N<sub>44</sub>O<sub>33</sub>S<sub>3</sub> (Cy3-**I**) (M + H<sup>+</sup>) 3304.57; found 3304.82. MALDI MS calculated for C<sub>170</sub>H<sub>235</sub>N<sub>43</sub>O<sub>39</sub>S<sub>3</sub> (Cy3-**II**) (M + H<sup>+</sup>) 3586.69; found 3587.84. MALDI MS calculated for C<sub>167</sub>H<sub>224</sub>N<sub>33</sub>O<sub>54</sub>S<sub>3</sub> (Cy3-**III**) (M + H<sup>+</sup>) 3639.50; found 3640.07. Extinction coefficients used to determine solution concentrations of Cy3-labeled **I–III** were ε<sub>280</sub> = 12 300 M<sup>-1</sup> cm<sup>-1</sup> and ε<sub>552</sub> = 150 000 M<sup>-1</sup> cm<sup>-1</sup> in water.

For Cy3-labeled **1–3**, HPLC elution was achieved with the following gradient: time 0, A/B = 100/0; 0–25 min, linear increase to A/B = 75/25; 25–27 min, linear change to A/B = 20/80; 27–37 min, A/B = 20/80. HPLC traces and retention times are provided in the Supporting Information. MALDI MS calculated for C<sub>97</sub>H<sub>161</sub>N<sub>44</sub>O<sub>21</sub>S<sub>3</sub> (Cy3-**1**) (M + H<sup>+</sup> - H<sub>2</sub>O) 2356.30; found 2357.68. MALDI MS calculated for C<sub>113</sub>H<sub>181</sub>N<sub>43</sub>O<sub>27</sub>S<sub>3</sub> (Cy3-**2**) (M + H<sup>+</sup> - 2H<sub>2</sub>O) 2632.29; found 2632.12. MALDI MS calculated for C<sub>110</sub>H<sub>170</sub>N<sub>33</sub>O<sub>42</sub>S<sub>3</sub> (Cy3-**3**) (M + H<sup>+</sup> - N<sub>2</sub>) 2697.12; found 2696.37. The concentration of Cy3-labeled peptides **1–3** in solution was determined using ε<sub>552</sub> = 150 000 M<sup>-1</sup> cm<sup>-1</sup>, and accounting for the fraction labeled. Cy3 labeling efficiency was determined using Ellman's reagent according to manufacturer's protocol.

**Cell Culture.** HFL-1 human diploid lung fibroblasts and AsPC-1 and CAPAN-2 human pancreatic carcinoma cell lines

were obtained from the Cell Culture Core of the Center for Molecular Studies in Liver and Digestive Diseases (University of Pennsylvania Medical School, Philadelphia, PA). NCI-H1975 cells were from Dr. Intae Lee and red blood cells were from Dr. Don Siegel (University of Pennsylvania Medical School, Philadelphia, PA). All cells were grown in 25 cm<sup>2</sup> tissue culture flasks in RPMI-1640 with 25 mM HEPES supplemented with 2 mM L-glutamine, 15% fetal calf serum, 100 units of penicillin, and 100 units of streptomycin. Cells were subcultured weekly, or more frequently, as needed.

**Cytotoxicity Assays.** In 96 well plates, 25 000 cells were plated per well and allowed to grow overnight. Nonfluorescently labeled peptide–cryptophane conjugates **I–III** were added from a stock solution in DPBS to wells in triplicate at final concentrations of 2, 10, 25, 50, 80, and 100 μM and incubated for 24 h in the dark. The medium was removed and the cells were washed thrice with DPBS before being treated with 20 μL of MTT for 3 h. The medium was removed once more and the resulting crystals were solubilized in DMSO. Absorbance at 540 nm was recorded in each well using the plate reader. Absorbance readings were subtracted from the value of wells containing untreated cells, and the reduction in cell growth was calculated as a percentage of control absorbance in the absence of any treatment. Data show the mean of at least three independent experiments ± SD.

**Cell Uptake Studies.** Cells were grown to confluence on LabTek 8-well microscope slides with glass coverslip bottoms. For uptake studies, cells were incubated with 2 μM solutions of Cy3-labeled **I**, **II**, or **III** for 15 min. For blocking studies, cells were pretreated for 45 min with an 100 μM solution of a cyclic RGDfV peptide containing D-phenylalanine that was previously identified to bind tightly to the integrin α<sub>v</sub>β<sub>3</sub> receptor (37, 38). In the antibody blocking studies, cells were pretreated for 30 min with 10 μM blocking anti-α antibody. For visualizing the results of both the uptake and blocking studies, the medium was removed and the cells were washed three times with DPBS. Cells were visualized using an Olympus FV1000 confocal laser scanning microscope with 543 nm (HeNe) laser excitation and Cy3 emission filter under 40× magnification (Olympus UApo/340 40×, 1.15 W).

**Time-Dependent Cellular Uptake.** Cells were plated at 10 000 cells per well in a CoStar 96-well plate and allowed to grow overnight. Cy3-labeled **I**, **II**, or **III** was added to the wells at a concentration of 10 μM and incubated for 0, 1, 2, 4, 8, and 24 h at 37 °C. At the end of the incubation time, the loading medium was removed, and the cells were washed thrice with DPBS. The cells were solubilized by the addition of 100 μL of 0.25% Triton X-100 in DPBS. To determine conjugate concentration, samples were excited at 544 nm and fluorescence at 590 nm was recorded using a plate reader. The cell numbers were then quantified using the CyQuant reagent (Molecular Probes) according to manufacturer protocol.

## RESULTS AND DISCUSSION

**Synthesis and Characterization of Peptide–Cryptophane Conjugates.** Monopropargylated cryptophane-A **4** was synthesized in 12 nonlinear steps and 3% overall yield (10). The yields of purified peptides (**1–3**) were 80–85% for all peptide coupling and cleavage steps, based on the maximum possible yield from starting resin. Azidopeptides, while still attached to the solid support, were reacted with **4** by a copper (I)-catalyzed [3 + 2] cycloaddition in 80–89% yield (39–41). Peptide–cryptophane conjugates (with Cys still protected) were cleaved from the resin, and purified by reverse-phase HPLC (Supporting Information Figures S1–S3). The cysteine was deprotected before use with TCEP to yield **I–III**. The deprotected cysteines showed no evidence of disulfide formation leading to cryptophane dimer-

ization on the time scale of hours when purified by HPLC. The free thiols, however, may interact with endogenous sulfhydryls when introduced into cells.

The (RGD)<sub>4</sub> linear peptide was chosen to target ABIR, because it was readily synthesized and attached to cryptophane using established protocols (10). Furthermore, polypeptides of similar length were found to confer excellent cryptophane water solubility. In contrast, the cryptophane-(RGD)<sub>4</sub> conjugate presented solubility problems, most likely due to charge interactions between the repeating sequence of arginine and glutamic acid residues. A prior version of conjugate **III** was synthesized without the PEG<sub>7</sub> linker separating the cryptophane from the RGD tetramer. This prototype exhibited poor water solubility, which prevented its usefulness for *in vitro* cell studies. Addition of the PEG<sub>7</sub> linker increased water solubility, allowing concentrations up to 120  $\mu$ M when DMSO (10% final concentration) was added to the buffer solutions.

The cysteine sulfhydryl group on the peptides and peptide-cryptophane conjugates was deprotected and reacted with maleimide-functionalized Cy3 to generate Cy3-labeled **1–3** and **I–III**. Mixtures of fluorescently labeled and unlabeled conjugates were obtained after reverse-phase HPLC purification (Supporting Information Figures S4–S6). For the cryptophane-peptide conjugates **I–III**, Cy3 labeling efficiencies of 50–69% were determined from the ratio of dye absorbance at 552 nm to the cryptophane absorbance at 280 nm. Cy3 labeling efficiencies were initially lower than expected. To improve yields, the reducing agent TCEP was removed from the solution by gel filtration chromatography before the addition of the Cy3 monoreactive dye pack. Removal of TCEP improved Cy3 conjugation yields by about 10%.

Ellman's reagent was used to determine the Cy3 labeling efficiencies for **1–3**, and confirmed the previous measurements determined for Cy3-labeled **I–III**. The 5,5'-dithiobis(2-nitrobenzoic acid) reacted with any free (previously unreacted) sulfhydryl groups to yield 2-nitro-5-thiobenzoic acid, which was quantified by measuring absorbance at 412 nm ( $\epsilon_{412} = 14\,150\text{ M}^{-1}\text{ cm}^{-1}$ ) (42). This assay found slightly higher Cy3 labeling efficiencies for **1–3** (60–72%) than for **I–III** (47–70%), which was in good agreement with the previously described ratiometric ( $A_{552}/A_{280}$ ) UV-vis measurements for Cy3-labeled **I–III**.

**Cell Toxicity Assays.** The cytotoxicity of the cryptophane conjugates was evaluated in AsPC-1, CAPAN-2, and HFL-1 cell lines by exposing cells to increasing concentrations of **I**, **II**, or **III** as shown in Figure 1. The (RGD)<sub>4</sub>-cryptophane conjugate **III** showed 25–30% proliferation inhibition of the various cell lines at the highest concentration studied (100  $\mu$ M). Slightly higher amounts of cytotoxicity were also found for the D-Arg<sub>9</sub>- and TAT-cryptophane conjugates, **I** and **II**, in both the AsPC-1 and CAPAN-2 cell lines. In general, the three conjugates appeared to be more toxic to HFL-1 fibroblast cells than either AsPC-1 or CAPAN-2 cancer cells. The toxicity profile is comparable to that of the similarly sized fullerene C<sub>60</sub> molecule, which decreased viability of HEK cells by 10–50% over a similar range of concentrations (43). For compound **III**, 50% inhibition of proliferation was not reached in any of the cell lines at the concentrations tested. Compounds **I** and **II** showed 50% inhibition at 60 and 75  $\mu$ M in HFL-1 fibroblasts. **I** also showed IC<sub>50</sub> of 75  $\mu$ M in AsPC-1 cells and more than 100  $\mu$ M in CAPAN-2. **II** had IC<sub>50</sub> values of 100  $\mu$ M in AsPC-1 cells, while 50% inhibition was not reached in CAPAN-2 cells at 100  $\mu$ M. Increased toxicity for compounds **I** and **II** as compared to **III** is thought to be a result of cryptophane delivery to the cell nucleus by TAT or D-Arg<sub>9</sub> nuclear localization peptides. For compound **III**, 10% DMSO was required to work at the higher concentrations. Cell viability assays for this compound were performed using 10% DMSO at all sample

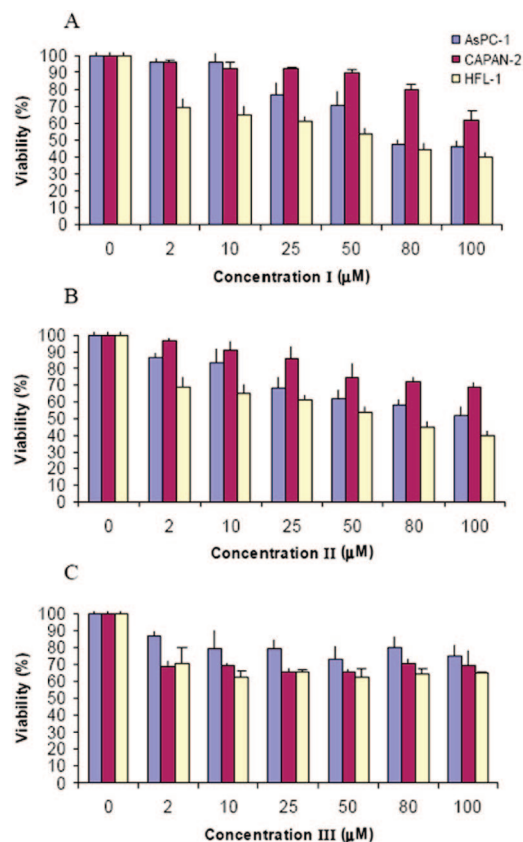


**Figure 1.** Cytotoxicity assay for conjugates **I** (A), **II** (B), and **III** (C) in AsPC-1 (blue), CAPAN-2 (maroon), and HFL-1 (off-white) cells. %Viability was determined via MTT assay after 24 h incubation with increasing concentrations of each conjugate, as compared to untreated cells.

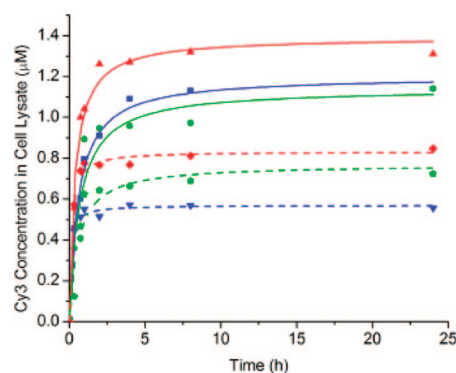


**Figure 2.** Uptake of peptides (solid lines) was measured for **1** (blue squares), **2** (red triangles), and **3** (green circles) and peptide-cryptophane conjugates (dashed lines) for **I** (blue inverted triangles), **II** (red diamonds), and **III** (green pentagons) by CAPAN-2 cells over 24 h.

concentrations, and these viability data were normalized to cells treated with 10% DMSO without cryptophane. In absolute terms, 10% DMSO alone reduced cell counts by 2000–3500, corresponding to a 8–14% decrease compared to untreated cells.

**Cell Uptake Studies.** The time-dependent uptake of Cy3-labeled peptide-cryptophane conjugates **I–III** and peptides **1–3** at 10  $\mu$ M was investigated in CAPAN-2 cells (Figure 2). All conjugates showed similar uptake kinetics with a rapid accumulation of compounds within the first hour. Maximum uptake was achieved by 4 h, and a plateau was observed for the remaining 20 h. In order to quantify cell uptake for each time point, 10 000 cells containing each fluorescent compound were placed in 100  $\mu$ L lysis buffer. The concentrations of

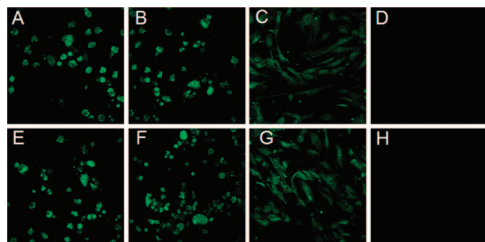


**Figure 3.** Cellular uptake of 2  $\mu\text{M}$  Cy3-labeled **I** (top row) and **II** (bottom row) in AsPC-1 (A,E), CAPAN-2 (B,F), and HFL-1 cells (C,G) after 1 h incubation at 37  $^{\circ}\text{C}$ . Uptake of **I** and **II** was inhibited after 1 h incubation at 4  $^{\circ}\text{C}$  (D,H).

fluorescent peptides and conjugates were quantified by fluorometry after generating a fluorescence standard curve for Cy3 in the same lysis buffer, and correcting for the Cy3-labeling efficiency of each compound. Fluorescent peptides **1–3** were measured in the cell lysate solution at concentrations of 1.0–1.4  $\mu\text{M}$ , whereas fluorescent cryptophane conjugates **I–III** were determined to be 500–800 nM. Within the error of the measurements, we cannot draw distinctions regarding the uptake efficiency of the three peptide motifs.

A procedure was developed to estimate the intracellular concentration of each compound from the lysate data. When detached from the surface, the CAPAN-2 cells were spherical and measured with a microscope to be  $\sim 35 \mu\text{m}$  in diameter. The average cell volume was calculated, and the fraction of the 100  $\mu\text{L}$  cell lysate originally occupied by the cells was determined to be 0.0050. Thus, the measured cell lysate concentrations of 500–800 nM gave an approximate range of intracellular concentrations of 100–160  $\mu\text{M}$  for **I–III** after the 24-h incubation period. This corresponds to 10–16-fold enrichment of **I–III** inside the cell (originally present in the media at 10  $\mu\text{M}$ ). Support for this finding comes from ratiometric measurements (Supporting Information Figures S7–S9) showing a range of fluorescence intensities that is 4–20 times greater inside the CAPAN-2 cells than the surrounding cell media. Importantly, these intracellular concentrations are within the limits of detection for laser-polarized  $^{129}\text{Xe}$  NMR experiments (43).

Confocal laser scanning microscopy (CLSM) confirmed cellular delivery of cryptophane with the D-Arg<sub>9</sub>- and TAT-cryptophane conjugates, **I** and **II** (Figure 3). After 1-h exposure to Cy3-labeled **I** and **II**, fluorescence was seen evenly distributed throughout most AsPC-1, CAPAN-2, and HFL-1 cells. Cy3-labeled **I** and **II** translocated into the cell nucleus, as was expected for conjugates of these peptides (45–47). After 1-h incubation at 4  $^{\circ}\text{C}$  with Cy3-labeled **I** and **II**, no fluorescence was observed (Figure 3D,H) by CLSM, which confirmed that uptake occurred via an energy-dependent endocytic pathway.

Cell uptake of Cy3-labeled **III** was also confirmed by CLSM. After 30-min incubation and rigorous cell washing, fluorescence was observed in NCI-H1975, CAPAN-2, and AsPC-1 cells (Figure 4A–C). Translocation of Cy3-labeled **III** was not observed in red blood cells, as expected, as these cells do not express  $\alpha_v\beta_3$  integrin receptor (Figure 4D). In contrast to Cy3-labeled **I** and **II**, Cy3-labeled **III** was not observed to cross the nuclear membrane. In general, nuclear internalization of imaging agents is undesirable because of potential mutagenic effects on healthy cells. To determine whether uptake of **III** was mediated by ABIR, cells were preincubated with 100  $\mu\text{M}$  cyclic RGDfV peptide, which is known to bind  $\alpha_v\beta_3$  integrin receptor with high affinity (48). Figure 4D shows that the cyclic RGDfV peptide inhibited uptake of (RGD)<sub>4</sub>-cryptophane as indicated by reduction in fluorescence. Internalization was also inhibited by coinubation with 10  $\mu\text{M}$  anti- $\alpha_v$  mouse antibody (Figure 4F). Cyclic RGDfV and anti- $\alpha_v$  mouse antibody blocking groups

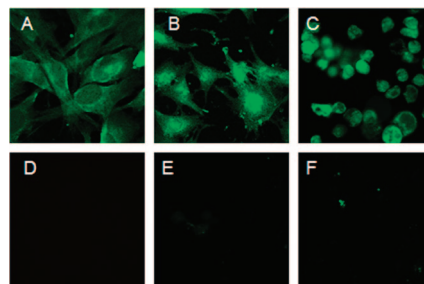


**Figure 4.** Uptake of 2  $\mu\text{M}$  Cy3-labeled **III** targeting  $\alpha_v\beta_3$  integrin in NCI-H1975 (A), HFL-1 (B), and CAPAN-2 (C) cells after 30 min incubation at 37  $^{\circ}\text{C}$ . Red blood cells (D) did not uptake this compound. Targeting in NCI-H1975 was successfully blocked with 100  $\mu\text{M}$  cyclic RGDfV peptide (E) and 10  $\mu\text{M}$  anti- $\alpha_v$  antibody (F).

also inhibited uptake in HFL-1 and CAPAN-2 cells (data not shown). These blocking data suggest that the (RGD)<sub>4</sub>-labeled conjugate was specifically recognized by the  $\alpha_v\beta_3$  integrin receptor and the  $\alpha_v$  subunit is critical for cellular uptake of **III**.

Attempts at performing hyperpolarized  $^{129}\text{Xe}$  NMR spectroscopy were made with compound **III** in isolated cells in culture. However, these experiments were unsuccessful due to the limited solubility of **III** and inability to achieve sufficient cell density within the detection volume. The requirement for incorporating DMSO in the buffers used to solubilize **III** further complicated the NMR data collection, as  $^{129}\text{Xe}$  NMR chemical shift is very sensitive to solvent composition. The requirement for DMSO also made it difficult to achieve the high density of viable cells required for these NMR experiments.

Conjugates **I–III** have molecular weights of 2500–3500 Da and their transport and clearance properties *in vivo* are not yet known. Fullerenes, which are similar in size and chemical composition, have been found to localize to a variety of tissues in rats with large accumulations in the liver, spleen, and kidneys, suggesting that these compounds are cleared rapidly (49, 50). PEG coatings may be used to improve bioavailability if the biodistribution of cryptophane is found to be similar to that of fullerene (51).

## CONCLUSION

Cryptophane-A was conjugated to (D-Arg)<sub>9</sub>, TAT, and (RGD)<sub>4</sub> peptides using a modified [3 + 2] cycloaddition reaction. This reaction provides a facile route for synthesizing chemically stable peptide-cryptophane conjugates (40, 52). All compounds were examined for cell toxicity, and fluorescently labeled with Cy3 to facilitate cellular imaging studies by CLSM.

Conjugates **I** and **II** were delivered nonspecifically to all cell types tested and showed little cytotoxicity in concentration ranges that are relevant for solution-based hyperpolarized  $^{129}\text{Xe}$  NMR experiments. Conjugate **III**, which contained an (RGD)<sub>4</sub>  $\alpha_v\beta_3$  integrin receptor binding motif, was selectively delivered to cells expressing this receptor and excluded from human red blood cells. **III** was similarly nontoxic as **I** and **II**. Importantly for laser-polarized  $^{129}\text{Xe}$  NMR studies, cryptophane concentrations in excess of 100  $\mu\text{M}$  were achieved in CAPAN-2 cells using the three peptides.

An important goal of these studies is to identify cell delivery motifs that can be attached to cryptophane and effectively discriminate between cancer and normal cells. The results of this initial study are very promising, and motivate the search for peptides and small molecules that promote the cellular delivery of even higher concentrations of cryptophanes, with reduced toxicity, in order to facilitate *in vivo* NMR studies. As examples, the transportan and penetratin CPP sequences were shown previously to deliver higher concentrations of attached cargo than TAT and (D-Arg)<sub>9</sub> peptides (53, 54). Additional cell

targeting motifs will be explored for use with other cancer biomarkers. Finally, protocols must be developed to perform  $^{129}\text{Xe}$  MRI experiments using xenon biosensors in tissue samples, where higher cellular density (and associated cryptophane per unit volume) will improve  $^{129}\text{Xe}$  MR signals. This work demonstrates that, due to their limited cytotoxicity and ready delivery to cells expressing specific cell surface receptors, cryptophanes offer considerable promise for in vivo xenon biosensing experiments.

#### ACKNOWLEDGMENT

We thank Intae Lee for providing cells and helpful discussions; Jeffery Saven, Ronen Marmorstein, and Scott Diamond for access to instrumentation; the Cell Culture Core of the University of Pennsylvania Center for Molecular Studies in Liver and Digestive Diseases for cells; Tobias Baumgart and Eric Meggers for access to cell culture facilities. This work was supported by the DOD (W81XWH-04-1-0657), NIH (1R21CA110104, 1R33CA110104, 1S10RR021113-01), and Camille and Henry Dreyfus Foundation.

**Supporting Information Available:** HPLC analysis of peptide–cryptophane conjugates I–III and Cy3-labeled peptides 1–3, and CLSM images of Cy3-labeled peptide 3 in CAPAN-2 cells. This material is available free of charge via the Internet at <http://pubs.acs.org>.

#### LITERATURE CITED

- Degani, H., Gusic, V., Weinstein, D., Feilds, S., and Strano, S. (1997) Mapping pathophysiological features of breast tumors by MRI at high spatial resolution. *Nat. Med.* 3, 780–782.
- Foster-Gareau, P., Heyn, C., Alejski, A., and Rutt, B. K. (2003) Imaging single mammalian cells with a 1.5 T clinical MRI scanner. *Magn. Reson. Med.* 49, 968–971.
- Golman, K., Zandt, R. I., Lerche, M., Pehrson, R., and Ardenkjaer-Larsen, J. H. (2006) Metabolic imaging by hyperpolarized  $^{13}\text{C}$  magnetic resonance imaging for in vivo tumor diagnosis. *Cancer Res.* 66, 10855–10860.
- Hopkins, S. R., Levin, D. L., Emami, K., Kadlecsek, S., Yu, J., Ishii, M., and Rizi, R. R. (2007) Advances in magnetic resonance imaging of lung physiology. *J. Appl. Physiol.* 102, 1244–1254.
- Mugler, J. P., Driehuys, B., Brookeman, J. R., Cates, G. D., Berr, S. S., Bryant, R. G., Daniel, T. M., deLange, E. E., Downs, J. H., Erickson, C. J., Happer, W., Hinton, D. P., Kassel, N. F., Maier, T., Phillips, C. D., Saam, B. T., Sauer, K. L., and Wagshul, M. E. (1997) MR imaging and spectroscopy using hyperpolarized Xe-129 gas: Preliminary human results. *Magn. Reson. Med.* 37, 809–815.
- Spence, M. M., Rubin, S. M., Dimitrov, I. E., Ruiz, E. J., Wemmer, D. E., Pines, A., Yao, S. Q., Tian, F., and Schultz, P. G. (2001) Functionalized xenon as a biosensor. *Proc. Natl. Acad. Sci. U.S.A.* 98, 10654–10657.
- Collet, A. (1996) Cryptophanes. *Comp. Supramol. Chem.* 2, 325–365.
- Hill, P. A., Wei, Q., Eckenhoff, R. G., and Dmochowski, I. J. (2007) Thermodynamics of xenon binding to cryptophane in water and human plasma. *J. Am. Chem. Soc.* 129, 9262–9263.
- Spence, M. M., Ruiz, E. J., Rubin, S. M., Lowery, T. J., Winsinger, N., Schultz, P. G., Wemmer, D. E., and Pines, A. (2004) Development of a functionalized xenon biosensor. *J. Am. Chem. Soc.* 126, 15287–15294.
- Wei, Q., Seward, G. K., Hill, P. A., Patton, B., Dimitrov, I. E., Kuzma, N. N., and Dmochowski, I. J. (2006) Designing Xe-129 NMR biosensors for matrix metalloproteinase detection. *J. Am. Chem. Soc.* 128, 13274–13283.
- Spence, M. M., Rubin, S. M., Dimitrov, I. E., Ruiz, E. J., Wemmer, D. E., Pines, A., Yao, S. Q., Tian, F., and Schultz, P. G. (2001) Functionalized xenon as a biosensor. *Proc. Natl. Acad. Sci. U.S.A.* 98, 10654–10657.
- Lowery, T. J., Garcia, S., Chavez, L., Ruiz, E. J., Wu, T., Brotin, T., Dutasta, J. P., King, D. S., Schultz, P. G., Pines, A., and Wemmer, D. E. (2006) Optimization of xenon biosensors for detection of protein interactions. *ChemBioChem* 7, 65–73.
- Ruiz, E. J., Sears, D. N., Pines, A., and Jameson, C. J. (2006) Diastereomeric Xe chemical shifts in tethered cryptophane cages. *J. Am. Chem. Soc.* 128, 16980–16988.
- Hilty, C., Lowery, T. J., Wemmer, D. E., and Pines, A. (2006) Spectrally resolved magnetic resonance imaging of a xenon biosensor. *Angew. Chem., Int. Ed.* 45, 70–73.
- Huber, G., Brotin, T., Dubois, L., Desvaux, H., Dutasta, J. P., and Berthault, P. (2006) Water soluble cryptophanes showing unprecedented affinity for xenon: Candidates as NMR-based biosensors. *J. Am. Chem. Soc.* 128, 6239–6246.
- Gupta, B., Levchenko, T. S., and Torchilin, V. P. (2005) Intracellular delivery of large molecules and small particles by cell-penetrating proteins and peptides. *Adv. Drug Delivery Rev.* 57, 637–651.
- Wright, L. R., Rothbard, J. B., and Wender, P. A. (2003) Guanidinium rich peptide transporters and drug delivery. *Curr. Protein Pept. Sci.* 4, 105–124.
- Goun, E. A., Pillow, T. H., Jones, L. R., Rothbard, J. B., and Wender, P. A. (2006) Molecular transporters: Synthesis of oligoguanidinium transporters and their application to drug delivery and real-time imaging. *ChemBioChem* 7, 1497–1515.
- Goun, E. A., Shinde, R., Dehnert, K. W., Adams-Bond, A., Wender, P. A., Contag, C. H., and Franc, B. L. (2006) Intracellular cargo delivery by an octaarginine transporter adapted to target prostate cancer cells through cell surface protease activation. *Bioconjugate Chem.* 17, 787–796.
- Sibirian-Vazquez, M., Jensen, T. J., Hammer, R. P., and Vicente, M. G. H. (2006) Peptide-mediated cell transport of water soluble porphyrin conjugates. *J. Med. Chem.* 49, 1364–1372.
- Yang, J. H., Wang, K., Driver, J., Yang, J. H., and Barron, A. R. (2007) The use of fullerene substituted phenylalanine amino acid as a passport for peptides through cell membranes. *Org. Biomol. Chem.* 5, 260–266.
- Belvisi, L., Bernardi, A., Colombo, M., Manzoni, L., Potenza, D., Scolastico, C., Giannini, G., Marcellini, M., Riccioni, T., Castorina, M., LoGiudice, P., and Pisano, C. (2006) Targeting integrins: Insights into structure and activity of cyclic RGD pentapeptide mimics containing azabicycloalkane amino acids. *Bioorg. Med. Chem.* 14, 169–180.
- Harris, T. D., Kalogeropoulos, S., Nguyen, T., Liu, S., Bartis, J., Ellars, C., Edwards, S., Onthank, D., Silva, P., Yalamanchili, P., Robinson, S., Lazewatsky, J., Barrett, J., and Bozarth, J. (2003) Design, synthesis, and evaluation of radiolabeled integrin  $\alpha(v)\beta(3)$  receptor antagonists for tumor imaging and radiotherapy. *Cancer Biother. Radiopharm.* 18, 627–641.
- Temming, K., Schiffelers, R. M., Molema, G., and Kok, R. J. (2005) RGD-based strategies for selective delivery of therapeutics and imaging agents to the tumour vasculature. *Drug Resist. Updates* 8, 381–402.
- Cescato, R., Schulz, S., Waser, B., Eltschinger, V., Rivier, J. E., Wester, H. J., Culler, M., Ginj, M., Liu, Q. S., Schonbrunn, A., and Reubi, J. C. (2006) Internalization of sst(2), sst(3), and sst(5) receptors: Effects of somatostatin agonists and antagonists. *J. Nucl. Med.* 47, 502–511.
- Ginj, M., Zhang, H. W., Waser, B., Cescato, R., Wild, D., Wang, X. J., Erchegyi, J., Rivier, J., Macke, H. R., and Reubi, J. C. (2006) Radiolabeled somatostatin receptor antagonists are preferable to agonists for in vivo peptide receptor targeting of tumors. *Proc. Natl. Acad. Sci. U.S.A.* 103, 16436–16441.
- Reubi, J. C., Eisenwiener, K. P., Rink, H., Waser, B., and Macke, H. R. (2002) A new peptidic somatostatin agonist with high affinity to all five somatostatin receptors. *Eur. J. Pharmacol.* 456, 45–49.

- (28) Hilgenbrink, A. R., and Low, P. S. (2005) Folate receptor-mediated drug targeting: From therapeutics to diagnostics. *J. Pharm. Sci.* **94**, 2135–2146.
- (29) Byzova, T. V., Goldman, C. K., Pampori, N., Thomas, K. A., Bett, A., Shattil, S. J., and Plow, E. F. (2000) A mechanism for modulation of cellular responses to VEGF: Activation of the integrins. *Mol. Cell* **6**, 851–860.
- (30) Byzova, T. V., Kim, W., Midura, R. J., and Plow, E. F. (2000) Activation of integrin  $\alpha(v)\beta(3)$  regulates cell adhesion and migration to bone sialoprotein. *Exp. Cell Res.* **254**, 299–308.
- (31) Cairns, R. A., Khokha, R., and Hill, R. P. (2003) Molecular mechanisms of tumor invasion and metastasis: An integrated view. *Curr. Mol. Med.* **3**, 659–671.
- (32) Felding-Habermann, B. (2003) Integrin adhesion receptors in tumor metastasis. *Clin. Exp. Metastas.* **20**, 203–213.
- (33) Pierschbacher, M. D., Hayman, E. G., and Ruoslahti, E. (1985) The cell attachment determinant in fibronectin. *J. Cell. Biochem.* **28**, 115–126.
- (34) Pierschbacher, M. D., and Ruoslahti, E. (1984) Cell attachment activity of fibronectin can be duplicated by small synthetic fragments of the molecule. *Nature* **309**, 30–33.
- (35) Ruoslahti, E. (2003) The RGD story: a personal account. *Matrix Biol.* **22**, 459–465.
- (36) Ruoslahti, E., and Pierschbacher, M. D. (1986) Arg-Gly-Asp - a versatile cell recognition signal. *Cell* **44**, 517–518.
- (37) Ye, Y. P., Bloch, S., Xu, B. G., and Achilefu, S. (2006) Design, synthesis, and evaluation of near infrared fluorescent multimeric RGD peptides for targeting tumors. *J. Med. Chem.* **49**, 2268–2275.
- (38) Gottschalk, K. E., and Kessler, H. (2002) The structures of Integrins and integrin-ligand complexes: Implications for drug design and signal transduction. *Angew. Chem., Int. Ed.* **41**, 3767–3774.
- (39) Tornøe, C. W., Christensen, C., and Meldal, M. (2002) Peptidotriazoles on solid-phase: [1,2,3]-Triazoles by regioselective copper(I)-catalyzed 1,3-dipolar cycloadditions of terminal alkynes to azides. *J. Org. Chem.* **67**, 3057–3064.
- (40) Punna, S., Kuzelka, J., Wang, Q., and Finn, M. G. (2005) Head-to-tail peptide cyclodimerization by copper-catalyzed azide-alkyne cycloaddition. *Angew. Chem., Int. Ed.* **44**, 2215–2220.
- (41) Rostovtsev, V. V., Green, L. G., Fokin, V. V., and Sharpless, K. B. (2002) A stepwise Huisgen cycloaddition process: Copper(I)-catalyzed regioselective "ligation" of azides and terminal alkynes. *Angew. Chem., Int. Ed.* **41**, 2596–2599.
- (42) Riddles, P. W., Blakeley, R. L., and Zerner, B. (1983) Reassessment of Ellman's reagent. *Methods Enzymol.* **91**, 49–60.
- (43) Rouse, J. G., Yang, J. Z., Barron, A. R., and Monteiro-Riviere, N. A. (2006) Fullerene-based amino acid nanoparticle interactions with human epidermal keratinocytes. *Toxicol. In Vitro* **20**, 1313–1320.
- (44) Lowery, T. J., Rubin, S. M., Ruiz, E. J., Spence, M. M., Winssinger, N., Schultz, P. G., Pines, A., and Wemmer, D. E. (2003) Applications of laser-polarized Xe-129 to biomolecular assays. *Magn. Reson. Imaging* **21**, 1235–1239.
- (45) Lindgren, M., Gallet, X., Soomets, U., Hallbrink, M., Brakenhielm, E., Pooga, M., Brasseur, R., and Langel, U. (2000) Translocation properties of novel cell penetrating transport and penetratin analogues. *Bioconjugate Chem.* **11**, 619–626.
- (46) Lindgren, M., Hallbrink, M., Prochiantz, A., and Langel, U. (2000) Cell-penetrating peptides. *Trends Pharmacol. Sci.* **21**, 99–103.
- (47) Zorko, M., and Langel, U. (2005) Cell-penetrating peptides: mechanism and kinetics of cargo delivery. *Adv. Drug Delivery Rev.* **57**, 529–545.
- (48) Haubner, R., Wester, H. J., Burkhart, F., Senekowitsch-Schmidtke, R., Weber, W., Goodman, S. L., Kessler, H., and Schwaiger, M. (2001) Glycosylated RGD-containing peptides, tracer for tumor targeting and angiogenesis imaging with improved biokinetics. *J. Nucl. Med.* **42**, 326–336.
- (49) Bolskar, R. D., Benedetto, A. F., Husebo, L. O., Price, R. E., Jackson, E. F., Wallace, S., Wilson, L. J., and Alford, J. M. (2003) First soluble M@C-60 derivatives provide enhanced access to metallofullerenes and permit in vivo evaluation of Gd@C-60[C(COOH)(2)](10) as a MRI contrast agent. *J. Am. Chem. Soc.* **125**, 5471–5478.
- (50) Xu, J. Y., Li, Q. N., Li, J. G., Ran, T. C., Wu, S. W., Song, W. M., Chen, S. L., and Li, W. X. (2007) Biodistribution of Tc-99m-C-60(OH)(x) in Sprague-Dawley rats after intratracheal instillation. *Carbon* **45**, 1865–1870.
- (51) Tabata, Y., and Ikada, Y. (1999) Biological functions of fullerene. *Pure Appl. Chem.* **71**, 2047–2053.
- (52) Rostovtsev, V. V., Green, L. G., Fokin, V. V., and Sharpless, K. B. (2002) A stepwise Huisgen cycloaddition process: Copper(I)-catalyzed regioselective "ligation" of azides and terminal alkynes. *Angew. Chem., Int. Ed.* **41**, 2596–2599.
- (53) Bendifallah, N., Rasmussen, F. W., Zachar, V., Ebbesen, P., Nielsen, P. E., and Koppelhus, U. (2006) Evaluation of cell-penetrating peptides (CPPs) as vehicles for intracellular delivery of antisense peptide nucleic acid (PNA). *Bioconjugate Chem.* **17**, 750–758.
- (54) Myrberg, H., Lindgren, M., and Langel, U. (2007) Protein delivery by the cell-penetrating peptide YTA2. *Bioconjugate Chem.* **18**, 170–174.